

Influence of moisture content on mode I fracture process of *Pinus pinaster*: evolution of micro-cracking and crack-bridging energies highlighted by bilinear softening in cohesive zone model

Ngoc Anh Phan¹ · Myriam Chaplain¹ ·
Stéphane Morel¹ · Jean-Luc Coureau¹

Received: 13 September 2016 / Published online: 13 April 2017
© Springer-Verlag Berlin Heidelberg 2017

Abstract This paper is dedicated to the study of the effect of moisture content on fracture properties of wood through the corresponding effect on the softening function used in cohesive zone model to describe quasi-brittle failure of wood. Bilinear softening parameters of cohesive zone model are estimated from equivalent linear elastic fracture mechanics resistance curve obtained from a significant number of fracture tests performed in mode I for a wide range of moisture contents (from 5 to 30% moisture). The evolution of the cohesive zone parameters as a function of the moisture exhibits a moisture dependence of the fracture properties of wood and especially the increase of the cohesive energy related to the crack-bridging phenomenon.

Introduction

Timber structures represent an interesting solution according to the environmental and ecological context. Nevertheless, the lifetime of timber structures is known to be dependent on the climatic conditions such as temperature and especially relative air humidity whose fluctuations may lead to the development of cracks in structural components. Therefore, the impact of moisture content on the fracture process of wood requires to be accurately investigated in order to better estimate the lifetime of timber structures. Since the pioneering work of Boström (1992) in which the progressive failure of wood was shown from the softening of the stress-displacement relationship estimated from tensile tests, wood is nowadays known to exhibit a quasi-brittle failure. Thus, the cracking of wood is preceded by the

✉ Ngoc Anh Phan
ngocanh.phan.gc@gmail.com

¹ Dépt. Génie Civil et Environnemental (GCE), Institut de Mécanique et d'Ingénierie - Bordeaux (I2M), Université de Bordeaux, UMR 5295, Bordeaux F-33000, France

development of a fracture process zone (FPZ) in which softening behaviors, such as micro-cracking and crack-bridging, take place. These cohesive phenomena lead to stress redistribution and energy dissipation contributing to the stabilization of the onset of the main crack propagation which is usually characterized by a resistance curve (R-curve) behavior (Bažant and Planas 1998; Morel et al. 2005, 2010; de Moura et al. 2008; Dourado et al. 2008; Dourado 2008; Coureau et al. 2013; Xavier et al. 2014a, b). Indeed, within the framework of equivalent linear elastic fracture mechanics (LEFM), the FPZ development ahead of the notch tip leads to a rising resistance to crack growth followed by a plateau resistance associated with the self-similar propagation of the main crack with its FPZ. With the exception of the equivalent LEFM which provides a useful approximation of the quasi-brittle fracture of wood through R-curve, only Non Linear Fracture Mechanics (NLFM) is able to describe such a behavior. Among NLFM models, cohesive zone models (CZM) are nowadays successfully applied to describe quasi-brittle fracture of wood (de Moura et al. 2008; Dourado et al. 2008; Dourado 2008; Morel et al. 2010; Xavier et al. 2014a, b). In this context, the FPZ is assumed to be confined into a cohesive interface, in which the material behavior is fully characterized by the predefined shape of a softening function. If the softening behavior related to quasi-brittle fracture is known to exhibit a concave shape, different approximations of this softening are studied (Fig. 1) and especially a linear shape (see de Moura et al. 2008; Xavier et al. 2014a) or a bi-linear one (see Coureau et al. 2006; Dourado et al. 2008; Morel et al. 2010).

According to Morel et al. (2010), a bi-linear approximation of the softening function (Fig. 1b) better exhibits the fracture behavior of quasi-brittle material (approximation of the concave function) and allows the description of the two main cohesive phenomena that are micro-cracking and crack-bridging (Fig. 1c) from their corresponding cohesive energies. The bi-linear softening function is characterized by four parameters (Fig. 1b): cohesive fracture energy G_f , critical crack opening w_c , tensile strength f_t and cohesive energy distribution $G_{f\mu}/G_f$ (i.e. ratio between the cohesive energy related to the micro-cracking phenomenon $G_{f\mu}$ and the total cohesive energy G_f).

Concerning the effect of moisture content of wood on its fracture properties, several studies have been dedicated to this subject but not all are analysed on the

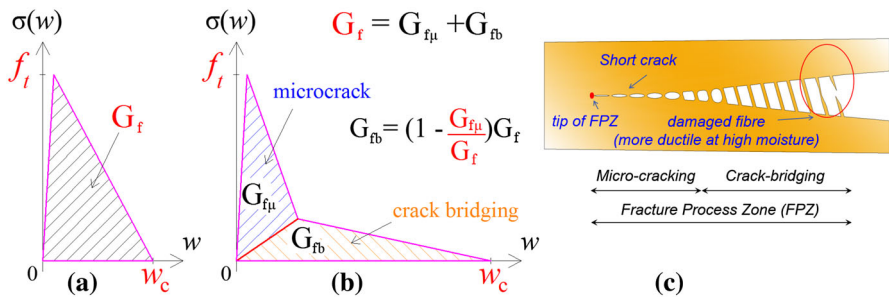


Fig. 1 a Linear softening function, b Bi-linear softening function, c Micro-cracking and crack-bridging in the FPZ

same mechanical basis. Thus, Prokopski (1996) and Reiterer and Stanzl-Tschegg (2002) analysed the fracture behavior of wood within the framework of LEFM (i.e. considering a negligible FPZ) and hence through its fracture toughness K_{Ic} or the average fracture energy G_F estimated from the energy corresponding to the area under the load-displacement response divided by the ligament area of the specimen. From Single Edge Notched (SEN) specimens of oak and pine considered at three moisture contents (6, 9 and 12%), Prokopski (1996) observed a decrease of the fracture toughness K_{Ic} of pine as a function of MC while the toughness of oak increased with MC. Later, Reiterer and Stanzl-Tschegg (2002) studied fracture properties of Maritime pine for four MC (7, 12, 18 and 55%) from Wedge Splitting Test (WST). They found that an increase of the average fracture energy G_F as a function of MC is associated with a higher ductility of the load-displacement response. The same trend was later confirmed by Vasic and Stanzl-Tschegg (2007) from in situ real time scanning electron microscopy during WST. They observed that higher moisture contents favor the tearing of wood cells at higher strain values and, consequently, at higher crack opening, leading to an increase of the average fracture energy G_F . More recently, in the framework of equivalent LEFM (leading to the estimation of R-curves) and using CZM, Xavier et al. (2014a) showed that the increase of moisture content (0–13%) of Maritime pine in RL configuration led to an increase of the cohesive energy G_f . Nevertheless, in spite of an estimated concave shape of the stress-opening relationship along the FPZ, Xavier et al. (2014a) used a linear approximation of the softening function and consequently could not conclude any evolution in distribution of cohesive energies between micro-cracking and crack-bridging cohesive phenomena.

Thus, as shown from the results of studies described above, the quasi-brittle fracture behavior of wood seems to be significantly influenced by moisture effect on the FPZ development and through the amount of dissipated energy in the FPZ. However, if it seems well established that an increase of moisture content leads to an increase of the cohesive fracture energy of wood, the distribution of this energy rising between the two main cohesive phenomena, micro-cracking and crack-bridging, remains to be established. In this respect, in spite of the use of recent experimental methods such as digital image correlation (Xavier et al. 2014a) or acoustic emission (Lamy et al. 2015), the direct observation of these cohesive phenomena and especially of their area of influence along the FPZ remains difficult. Nevertheless, this difficulty can be overcome thanks to cohesive zone model, in using the bi-linear approximation of the softening function from which the cohesive energies related to micro-cracking and crack-bridging phenomena are explicitly separated (Fig. 1).

In this paper, in order to study the moisture effect on the fracture behavior of wood, quasi-static mode I fracture tests are performed from Maritime pine modified Tapered Double Cantilever Beam specimens for a wide range of moisture contents. For each fracture test, the CZ parameters describing the bi-linear softening function are estimated from the equivalent LEFM R-curve. The observed evolution of cohesive zone parameters as a function of moisture content allows to discuss the moisture effect on fracture process of wood.

Quasi-static mode I fracture tests

Quasi-static mode I fracture tests are performed on Maritime pine (*Pinus pinaster Ait*) modified Tapered Double Cantilever Beam (mTDCB) specimen shown in Fig. 2. This specimen geometry favors the stability of the crack growth in the tapered part (zone 1) of the specimen. The initial crack length ($a_0 = 40$ mm) is machined with a band saw (thickness 1 mm) and prolonged a few millimeters with a sharp blade. The ligament length of the specimen is $d = 225$ mm and the relative initial notch length corresponds to $\alpha_0 = a_0/d = 0.18$. Fracture tests are performed according to TL configuration of wood. The average density of wood is estimated equal to 0.515 ± 0.040 g/cm³ at 12% moisture content (MC).

Three hundred mTDCB specimens are manufactured and stored in a climatic room at ten different air relative humidity (RH) and at 20°C in order to obtain 10 corresponding moisture contents of the specimens: 5, 8, 10, 12, 15, 18, 20, 22, 25 and 30%. The conditioning time evolves from 2 to 10 weeks as a function of the expected value of MC. The moisture content of a specimen is reached when the specimen weight remains unchanged during 2 days, with a reasonable tolerance (0.05 g).

Image processing method is used to obtain the relative displacement between the points P_1 and P_2 (Fig. 2) which is considered as representative of the displacement of the load P . During experimental tests, load-displacement data are recorded with a frequency close to 10 Hz. On the other hand, in order to minimize the viscoelastic effects and the change of moisture content during the fracture tests, the complete fracture of each specimen is carried out in 3 ± 1 min which corresponds to a velocity of the imposed displacement ranges from 1 mm/min for MC close to 5% up to 2 mm/min for MC close to 30%.

Equivalent LEFM : R-Curve

Equivalent LEFM

Equivalent LEFM is known to be applicable to moisture content of wood around 12% (Morel et al. 2005; de Moura et al. 2008; Dourado et al. 2008; Dourado 2008;

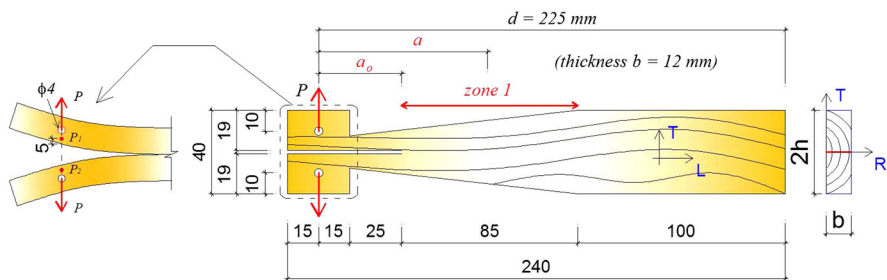


Fig. 2 mTDCB specimen geometry (dimensions in mm)

Morel et al. 2010; Coureau et al. 2013; Xavier et al. 2014a, b). However, its application to a large range of moisture content (especially for high moisture) has never been checked.

In order to check the validity of the equivalent LEFM approach for each moisture content, loading-unloading cycles are carried on specimens according to the procedure detailed by Morel et al. (2005). Typical cycles obtained for 12% MC and 30% MC are shown in Fig. 3. The results show that the initial compliance of a given cycle, i.e. the elastic compliance of the specimen, corresponds to the secant compliance related to the unloading point of the preceding cycle. Note that such a phenomenon has been observed for all moisture contents considered in this study (i.e. ranged between 5 and 30%) and hence it can be argued that the secant compliance provides an estimation of the elastic compliance of the specimen for all moisture content corresponding to the hygroscopic domain of wood. Thus, the quasi-brittle fracture of wood (i.e. FPZ development ahead of the notch tip followed by the propagation of the main crack with its FPZ) induces only an increase of the elastic specimen compliance (without existence of irreversible displacement) which can be estimated from the secant compliance related to any point of the load-displacement response.

The fact that the fracture behavior of wood leads only to an increase of the specimen compliance (i.e. without irreversible displacement) is in agreement with the framework of equivalent LEFM from which the *equivalent LEFM crack length* will have to be estimated from any point of the load-displacement response from the corresponding secant compliance.

However, the estimation of the equivalent LEFM crack length requires the knowledge of the compliance function. In this study, the compliance function is estimated from a finite element analysis (FEA). The full geometry of the specimen is meshed as shown in Fig. 4 in order to take into account the effects of the crack tip

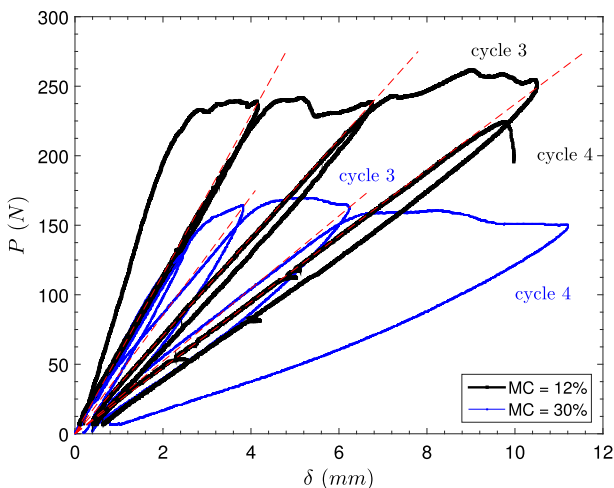


Fig. 3 Typical load-unloading cycles test. The *straight lines* correspond to the initial stiffness of each cycle and are consistent with the secant compliance related to the unloading point of the preceding cycles

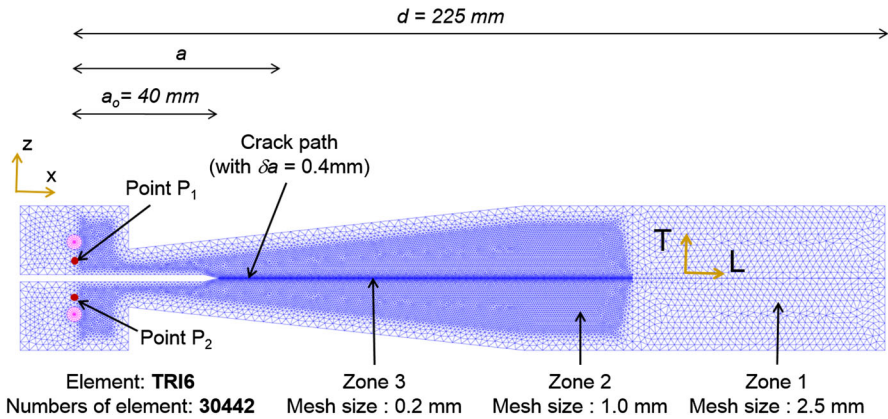


Fig. 4 Mesh of the mTDCB specimen used in FE analysis (elastic analysis and CZ simulations)

Table 1 Elastic properties of Maritime pine at 12% MC (Guitard 1987)

$E_L^{12\%}$ (MPa)	$E_T^{12\%}$ (MPa)	$G_{LT}^{12\%}$ (MPa)	ν_{TL}
13,500	1054	1094	0.425

rotation and those linked to the shear at the crack tip. The elastic properties of Maritime pine at 12% MC are reported in Table 1 and the variation of the elastic properties as a function of moisture content (MC) is estimated from the expression proposed by Guitard (1987) such as :

$$\begin{cases} E_L(MC) = E_L^{12\%} [1 - 0.015(MC - 12)] \\ E_T(MC) = E_T^{12\%} [1 - 0.030(MC - 12)] \\ G_{LT}(MC) = G_{LT}^{12\%} [1 - 0.030(MC - 12)] \end{cases} \quad (1)$$

Note that, according to Eq. (1), Poisson ratio is consequently considered to be independent of the moisture content. From the FE analysis, the compliance function is computed as :

$$\lambda(a) = \delta/P \quad (2)$$

where a is the crack length, δ corresponds to the relative displacement between points P_1 and P_2 (Fig. 4) which are in agreement with the points considered experimentally (Fig. 2) and P is the applied load.

In practice, due to the approximation of the elastic properties used in FE analysis compared to experimental ones, experimental and numerical compliance functions are different one from each other. In order to establish the correspondence between the numerical compliance $\lambda(a)$ and the experimental one $\lambda_{exp}(a)$, a multiplicative correction of the numerical compliance can be performed (Morel et al. 2005) such as:

$$\lambda_{\text{exp}}(a) = \psi \lambda(a) \quad (3)$$

where ψ corresponds to the correction factor and can only be estimated from the experimental and numerical compliances corresponding to the initial notch length for which actual crack length and equivalent LEFM one lead to the same value a_0 :

$$\psi = \frac{\lambda_{\text{exp}}(a_0)}{\lambda(a_0)} \quad (4)$$

Note that the reliability of this multiplicative correction of the compliance function has been accurately studied by Phan (2016) considering variation of elastic properties E_L, E_T and G_{LT} . It has been shown that such a correction provides an approximation of the actual compliance function with a reasonable accuracy (Phan 2016).

Equivalent LEFM : crack growth resistance curve (R-curve)

The first step of the equivalent LEFM approach is to estimate the equivalent crack length corresponding to each point of the experimental load-displacement response. In practice, for a given point of the load-displacement curve (P, δ), the equivalent LEFM crack length a (called *crack length* in the following for the sake of simplicity) is obtained from the corrected compliance function [Eq. (3)] in identifying the crack length a which gives the same compliance value as the experimental secant compliance corresponding to the considered point. On this basis, the resistance to crack growth $G_R(a)$ can be estimated from the energy release rate $G(a)$ such as:

$$G_R(a) = G(a) = \frac{P^2}{2b} \frac{\partial \lambda(a)}{\partial a} \quad (5)$$

where P is the applied load, b is the specimen thickness and $\lambda(a)$ is the corrected compliance function.

The typical R-curves obtained from the load-displacement responses corresponding to 8, 12 and 30% MC are plotted in Fig. 5. The R-curves corresponding to

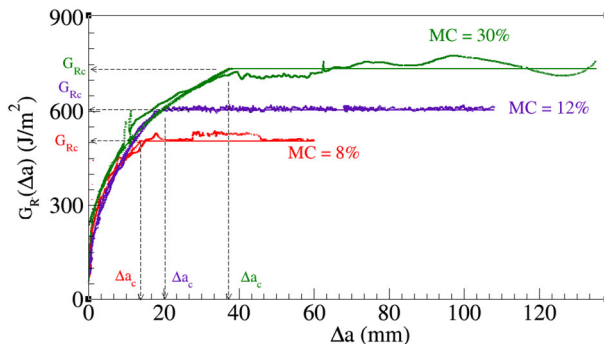


Fig. 5 Typical load-displacement curves obtained for the moisture content values 8, 12 and 30%

the other moisture contents are not plotted in Fig. 5 for clarity reason. All the R-curves exhibit a first zone where the resistance to crack growth increases as a function of the equivalent LEM crack length followed by a second regime for which the resistance to crack growth remains constant as expected for a self-similar crack propagation. In fact, the rising resistance zone is well known to be associated with the FPZ development ahead of the notch tip while the plateau resistance regime is linked to the self-similar propagation of the main crack with its FPZ (Morel et al. 2005, 2010; de Moura et al. 2008; Durado et al. 2008; Durado 2008; Coureau et al. 2013; Xavier et al. 2014a, b). These two regimes of the resistance to crack growth symptomatic of the quasi-brittle failure can be fitted by an analytical function expressed as a function of the equivalent LEM crack length increment $\Delta a = a - a_0$ (where a_0 corresponds to the initial notch length) defined as:

$$G_R(\Delta a) = \begin{cases} \frac{G_{Rc}}{\Delta a_c^\beta} \Delta a^\beta & \text{if } \Delta a < \Delta a_c \\ G_{Rc} & \text{if } \Delta a \geq \Delta a_c, \end{cases} \quad (6)$$

where $\Delta a_c = a_c - a_0$ corresponds to the equivalent LEM crack length increment for which the regime of the plateau resistance occurs, G_{Rc} is the plateau resistance and β is the exponent of the power law describing the rising resistance regime. Note that Δa_c provides an estimation of the equivalent LEM length of the FPZ and is usually called *internal length* in quasi-brittle failure.

All the R-curves have been fitted according to Eq. (6) and the average of the results obtained for each moisture content is reported in Table 2. In this Table, the evolution of the R-curve parameters confirms an increase of the plateau resistance G_{Rc} with the rise of moisture as expected from the previous studies of Reiterer and Stanzl-Tschegg (2002), Vasic and Stanzl-Tschegg (2007) and Xavier et al. (2014a). The increase of the plateau resistance (which corresponds to the resistance related to the self-similar propagation of the main crack with its FPZ) is also associated with an increase of the equivalent LEM length of the FPZ Δa_c . These last two results emphasize that the increase of the moisture content in the material leads to a rising

Table 2 R-curve parameters estimated for 10 moisture contents: mean and standard deviation in brackets

MC (%)	Number of specimens	G_{Rc} (J/m ²)	Δa_c (mm)	β
4.96 (0.35)	28	477 (58)	10.0 (4.0)	0.235 (0.053)
7.93 (0.38)	20	503 (62)	13.1 (3.8)	0.233 (0.048)
9.89 (0.42)	31	538 (52)	18.6 (5.6)	0.239 (0.040)
11.85 (0.72)	30	599 (52)	18.7 (5.5)	0.272 (0.049)
15.16 (0.53)	24	643 (54)	24.5 (4.5)	0.301 (0.037)
18.14 (0.63)	19	693 (48)	27.5 (5.2)	0.383 (0.039)
19.91 (0.58)	28	725 (46)	26.9 (5.5)	0.428 (0.032)
22.05 (0.64)	17	742 (61)	29.4 (3.7)	0.437 (0.043)
25.33 (0.66)	25	748 (62)	30.2 (5.1)	0.407 (0.044)
29.63 (1.20)	33	752 (64)	28.1 (5.7)	0.396 (0.047)

of the FPZ size and a corresponding increase of the resistance to crack growth of the main crack.

Cohesive zone model: bi-linear approximation of the softening

As shown by Morel et al. (2010), the R-curve is bijectively related to the softening behavior of the material. In particular, when the R-curve is described according to Eq. (6) and the softening behavior approximated by a bi-linear function, connections can be established between the R-curves parameters and those used to describe the bi-linear softening function. Thus, as schematically illustrated by Coureau et al. (2013) in Fig. 6, Morel et al. (2010) have shown that (i) the critical cohesive energy

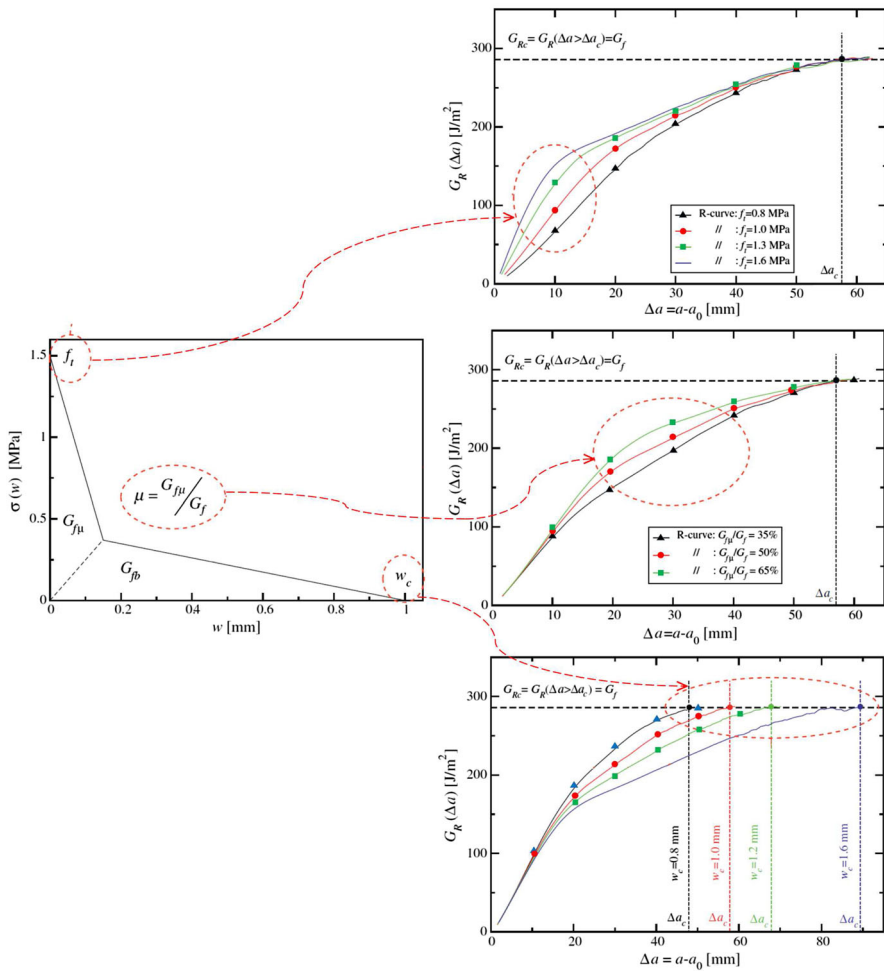


Fig. 6 Sketch of the connections between the bi-linear softening function used in CZM function and the corresponding R-curve (extracted from Coureau et al. 2013)

Table 3 Cohesive zone parameters (bi-linear softening) obtained for 10 moisture contents (standard deviation is given in brackets)

MC (%)	Number of specimens	G_f (J/m ²)	w_c (mm)	f_t (MPa)	$G_{f\mu}/G_f$
4.96 (0.35)	28	477 (58)	0.27 (0.10)	6.21 (0.40)	0.630 (0.033)
7.93 (0.38)	20	503 (62)	0.38 (0.09)	5.18 (0.38)	0.618 (0.048)
9.89 (0.42)	31	538 (52)	0.57 (0.14)	4.40 (0.32)	0.613 (0.034)
11.85 (0.72)	30	599 (52)	0.64 (0.17)	3.88 (0.38)	0.587 (0.038)
15.16 (0.53)	24	643 (54)	0.90 (0.16)	3.24 (0.27)	0.509 (0.036)
18.14 (0.63)	19	693 (48)	1.03 (0.19)	2.68 (0.32)	0.459 (0.052)
19.91 (0.58)	31	725 (46)	1.14 (0.25)	2.29 (0.31)	0.397 (0.055)
22.05 (0.64)	17	742 (61)	1.25 (0.17)	2.13 (0.23)	0.364 (0.036)
25.33 (0.66)	25	748 (62)	1.35 (0.24)	2.13 (0.32)	0.291 (0.050)
29.63 (1.20)	33	752 (64)	1.35 (0.28)	2.09 (0.27)	0.287 (0.052)

G_f is equal to the plateau resistance G_{Rc} , (ii) the critical crack opening w_c has a direct influence on the equivalent LEFM length of the FPZ Δa_c (i.e. the length of the rising part of the R-curve), (iii) the tensile strength f_t influences the magnitude of the resistance to crack growth in the initial part of the R-curve while (iv) the cohesive energy ratio $G_{f\mu}/G_f$ mainly influences the magnitude of the resistance in the central part of the R-curve. However, due to the fact that both f_t and $G_{f\mu}/G_f$ have an influence on the magnitude of the rising part of the R-curve, a step by step procedure was proposed by Morel et al. (2010) in order to decouple the effects of these CZ parameters and thus obtain the single set of cohesive parameters corresponding to the one to one correspondence between the R-curve and the softening function.

Based on the bijective relation between the R-curve and the cohesive zones parameters and according to the step by step procedure proposed by Morel et al. (2010), an automated identification procedure has been established (Phan 2016) allowing the estimation of the CZ parameters (G_f, w_c, f_t and $G_{f\mu}/G_f$) of each experimental test. The average of each CZ parameter obtained as a function of moisture content is reported in Table 3.

The information provided by the evolution of the CZ parameters as a function of MC on the fracture process of wood is discussed in the following section.

Moisture content effects on wood fracture process

Moisture content effect on the cohesive energy distribution

As previously mentioned (i.e. $G_f = G_{Rc}$), the increase of the plateau resistance G_{Rc} of the R-curve (Table 2) leads to a corresponding increase of the cohesive energy G_f as a function of moisture (Table 3; Fig. 7). Thus, as expected from previous studies (Reiterer and Stanzl-Tschegg 2002; Vasic and Stanzl-Tschegg 2007; Xavier et al.

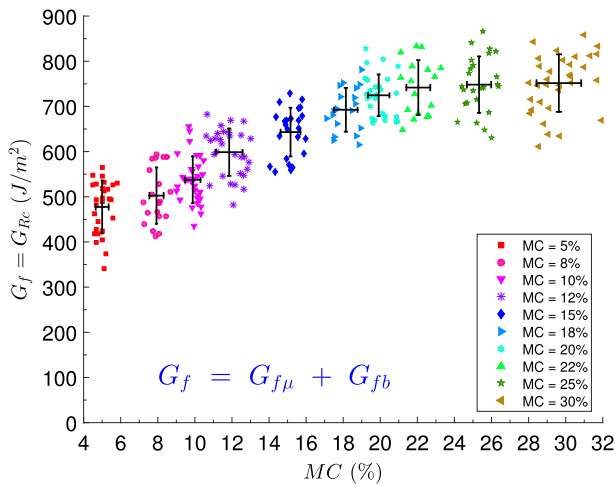


Fig. 7 Cohesive energy G_f as a function of moisture content. The *error bars* indicate the standard deviation: *vertical bars* correspond to the standard deviation of G_f , while *horizontal ones* represent the standard deviation of MC

2014a), with increasing moisture content, more fracture energy is required to completely fracture the specimens.

For all considered moisture contents, the mean value of G_f ranged from 477 to 752 J/m², which are two or three times higher than those obtained by Reiterer and Stanzl-Tschegg (2002), Vasic and Stanzl-Tschegg (2007) and Xavier et al. (2014a). However, one considers here the cohesive fracture energy (which is equal to the plateau resistance of the R-curve) while Reiterer and Stanzl-Tschegg (2002) and Vasic and Stanzl-Tschegg (2007) considered the average fracture energy G_f (which is computed from the total work of fracture divided by the whole ligament area of the specimen). In the same way, Xavier et al. (2014a) found a variation of the cohesive energy G_f from 100 to 350 J/m² in the range of MC 0–13%. These differences of cohesive energy values may be due to the use of different specimen geometry as well as to differences linked to the wood species. Nevertheless, note that the ratio between the highest value of G_f and the smallest one is here equal to 1.58 and is in agreement with those obtained in the studies of Reiterer and Stanzl-Tschegg (2002) and Vasic and Stanzl-Tschegg (2007).

Moreover, as shown in Fig. 7, the cohesive fracture energy G_f increases until MC reaches approximately 25% and then remains stable for moisture higher than 25–30%. This behavior is in agreement with the expected upper limit of the hygroscopic domain of wood ($\approx 30\%$).

On the other hand, the moisture-dependent character of the cohesive energy is associated with an evolution of both main components of the cohesive energy: micro-cracking and crack-bridging energies. Indeed, as shown in Table 3, the ratio $G_{f\mu}/G_f$ related to the cohesive energy distribution exhibits a decrease with the increase in moisture. Knowing the evolution of the cohesive energy G_f and of the cohesive energy distribution $G_{f\mu}/G_f$ as a function of MC , it is easy to show that the

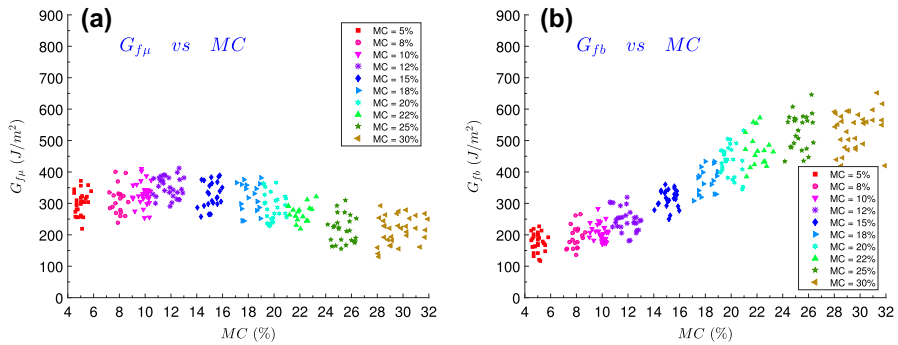


Fig. 8 **a** Micro-cracking cohesive energy G_{fm} and **b** Crack-bridging cohesive energy G_{fb} as a function of moisture content

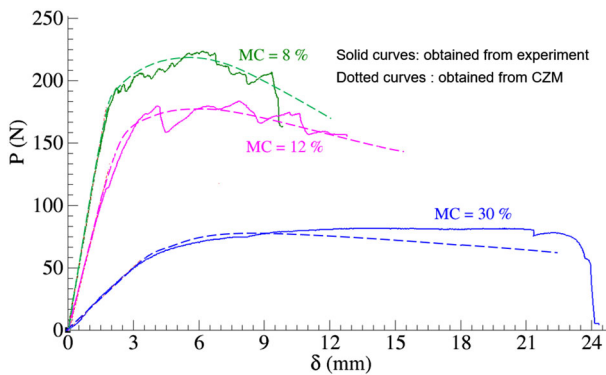


Fig. 9 Typical load-displacement responses obtained for the moisture content values 8%, 12% and 30%, and their corresponding simulations from CZM

micro-cracking cohesive energy G_{fm} remains approximately constant as a function of moisture content as shown in Fig. 8a, while the component of the fracture energy related to the crack bridging phenomenon G_{fb} exhibits an increase as a function of MC (Fig. 8b).

From Fig. 8a, b, it can be argued that crack-bridging mechanism governs the failure in mode I for wet wood, whereas this mechanism is less important for dried wood. This latter result is also in agreement with the trend of moisture content to promote crack bridging mechanism observed by Vasic and Stanzl-Tschegg (2007) from scanning electron microscopy during wedge-splitting test. Moreover, the enhancement of the crack-bridging mechanism as a function of MC leads to an increase of the ductility of the load–displacement response as shown in Fig. 9.

Note that, the load-displacement responses obtained from CZM are also plotted in Fig. 9 for example. As observed from the experimental responses, the simulated load-displacement responses also exhibit an increase of the response ductility as a function of MC.

Effect on the cohesive zone length (FPZ length)

Figure 10a, b show respectively the bilinear softening functions described in Table 3 expected for the 10 moisture contents values and their corresponding normal stress distributions along the cohesive interface corresponding to the state of the fully developed FPZ (i.e. at the onset of the self-similar propagation of the stress-free crack). On the basis of the stress distribution along the cohesive interface, the critical length of the cohesive zone l_{coh}^c is defined as the distance between positions of the points A and C (Fig. 10b) where the point A corresponds to the point for which the stress is equal to the tensile strength f_t while the point C is the point for which the crack opening reaches the critical value w_c and hence a nil stress.

Figure 11 illustrates the evolution of the critical length l_{coh}^c versus moisture. It can be seen that the critical length l_{coh}^c increases with the rise of MC. Thus, the critical length of the cohesive zone is longer in wet wood than in dried wood. This result is in agreement with the evolution of the equivalent LFM length of the FPZ Δa_c as a function of MC observed from the R-curves and given in Table 2.

Finally, similarly to the critical cohesive energy G_f , the critical crack opening w_c has a tendency to increase with the moisture until 25% and then remains stable for higher values of MC (Table 3). The average critical crack opening w_c obtained in this work varies from 0.3 to 1.4 mm from dry to wet wood. In previous studies (Dourado et al. 2010; Xavier et al. 2014a), using a linear softening function for DCB pine specimen, w_c has been found equal to 0.06 mm. Such a difference may be related to the use of different specimen geometry, different specimen size and especially, to different softening law used in CZM: linear function used by Dourado

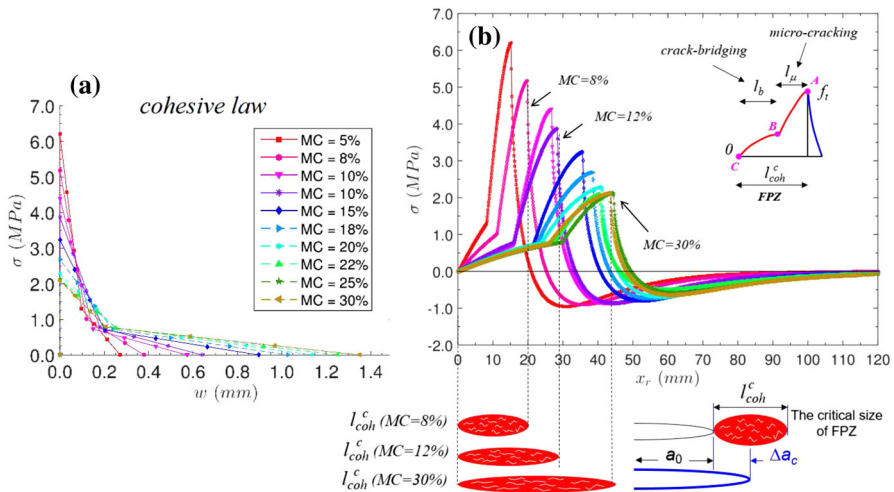


Fig. 10 a Softening functions plotted from CZ parameters reported in Table 3 corresponding to 10 MC and b Evolution of normal stresses along the cohesive interface for each MC value. The abscissa x_r along the cohesive interface is considered from the tip of the stress-free crack

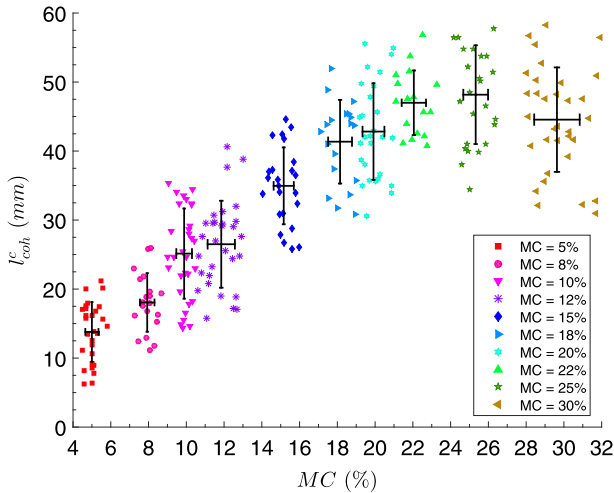


Fig. 11 Critical length of the cohesive zone l_{coh}^c versus moisture content. The *error bars* indicate the standard deviation: *vertical bars* correspond to the standard deviation of l_{coh}^c while *horizontal ones* represent the standard deviation of MC

et al. (2010) and Xavier et al. (2014a) while a bi-linear function is used in the present study.

To sum up, the fracture process of wood appears as moisture-dependent. With the increase of MC, the crack bridging mechanism becomes preponderant while the intensity linked to micro-cracking phenomenon remains approximately constant whatever MC is. Moreover, the increase of crack bridging (fibre bridging) and especially, of the associated cohesive energy lead to a rising of the FPZ length and to large opening of the FPZ. Both latter evolutions lead to an increase of the fracture energy and favor the stability of the propagation of the main crack, inducing a relative ductility of the load-displacement response of wood at failure.

Conclusion

The influence of the moisture content on the fracture behavior (mode I) of Maritime pine is investigated from a large campaign of fracture tests performed from mTDCB specimens. Approximately 300 fracture tests are carried out for 10 moisture content values ranging between 5 and 30%. Each fracture test is analyzed within the framework of equivalent LEFM and the R-curves obtained allow an estimation of the cohesive zone parameters describing the bilinear approximation of the softening function used in CZM according to the step by step procedure proposed by Morel et al. (2010). The results show that the fracture behavior of wood strongly depends on the moisture content. For moisture content value lower than 25%, the cohesive energy G_f , the critical opening w_c and hence the critical length of the cohesive zone (FPZ) increase with moisture content. Conversely, the tensile strength f_t and the cohesive energy distribution ratio $G_{f\mu}/G_f$ decrease with the increasing moisture

content. For moisture content value higher than 25%, all the cohesive zone parameters exhibit a relative independence with respect to MC. On this basis, from the estimation of the evolution of the cohesive energies associated with the micro-cracking and crack-bridging phenomena, it is shown that the crack-bridging mechanism becomes preponderant with the increase of MC while the intensity of the micro-cracking phenomenon remains approximately constant. The increase of the cohesive energy related to the one of the crack-bridging mechanism leads to a rising of the maximum opening of the cohesive zone as well as to longer critical cohesive zone. Larger cohesive zone associated with higher cohesive energy and critical opening of the cohesive interface observed with the increase of moisture content favors the stability of the propagation of the main crack and induces a relative ductility of the load-displacement response of wood at failure.

Acknowledgements The authors thank the French National Research Agency (ANR) for supporting the study through the Xyloplate project, Equipex XYLOFOREST (ANR-10-EQPX-16). This work is also supported by the Regional Council of Aquitaine and by the CODIFAB. Computational aspects of the study were performed at MCIA (Mésocentre de Calcul Intensif Aquitain) of the Université de Bordeaux and of the Université de Pau et des Pays de l'Adour.

References

- Bažant ZP, Planas J (1998) Fracture and size effect in concrete and other quasibrittle materials. CRC Press, Boca Raton
- Boström L (1992) Method for determination of the softening behaviour of wood and the applicability of a nonlinear fracture mechanics model. PhD thesis, University of Lund
- Coureau JL, Morel S, Gustafsson PJ, Lespine C (2006) Influence of the fracture softening behaviour of wood on load-COD curve and R-curve. *Mater Struct* 40(1):97–106
- Coureau JL, Morel S, Dourado N (2013) Cohesive zone model and quasibrittle failure of wood: a new light on the adapted specimen geometries for fracture tests. *Eng Fract Mech* 109:328–340
- de Moura M, Morais J, Dourado N (2008) A new data reduction scheme for mode I wood fracture characterization using the double cantilever beam test. *Eng Fract Mech* 75(13):3852–3865
- Dourado N (2008) R-Curve behaviour and size effect of a quasibrittle material: wood. PhD thesis, Université de Bordeaux I
- Dourado N, Morel S, de Moura M, Valentin G, Morais J (2008) Comparison of fracture properties of two wood species through cohesive crack simulations. *Compos Part A Appl Sci Manuf* 39(2):415–427
- Dourado N, de Moura M, Morais J, Silva M (2010) Estimate of resistance-curve in wood through the double cantilever beam test. *Holzforschung* 64(1):119–126
- Guitard D (1987) Mécanique matériau bois et composites (Mechanics of wood and composites materials). Cepadues Editions, France
- Lamy F, Takarli M, Angellier N, Dubois F, Pop O (2015) Acoustic emission technique for fracture analysis in wood materials. *Int J Fract Mech* 192:57–70
- Morel S, Dourado N, Valentin G, Morais J (2005) Wood: a quasibrittle material R-curve behavior and peak load evaluation. *Int J Fract* 131(4):385–400
- Morel S, Coureau JL, Planas J, Dourado N (2010) Bilinear softening parameters and equivalent LEFM R-curve in quasibrittle failure. *Int J Solids Struct* 47(6):837–850
- Phan NA (2016) Simulation of time-dependent crack propagation in a quasi-brittle material under relative humidity variations based on cohesive zone approach : application to wood. PhD thesis, University of Bordeaux
- Prokopski G (1996) Influence of moisture content on fracture toughness of wood. *Int J Fract* 79(4):R73–R77
- Reiterer A, Stanzl-Tschegg SE (2002) The influence of moisture content on the mode I fracture behaviour of sprucewood. *J Mater Sci* 37:4487–4491

- Vasic S, Stanzl-Tschegg SE (2007) Experimental and numerical investigation of wood fracture mechanisms at different humidity levels. *Holzforschung* 61(4):367–374
- Xavier J, Monteiro P, Morais J, Dourado N, de Moura M (2014a) Moisture content effect on the fracture characterisation of *Pinus pinaster* under mode I. *J Mater Sci* 49(21):7371–7381
- Xavier J, Oliveira M, Monteiro P, Morais J, de Moura M (2014b) Direct Evaluation of Cohesive Law in Mode I of *Pinus pinaster* by Digital Image Correlation. *Exp Mech* 54:829–840